An experimental investigation of oscillatory viscous flow in pipe bends

by

Arnold F. Bertelsen and Leif K. Thorsen

Abstract

Oscillatory flow in U-shaped pipes have been investigated experimentally. The velocity field is mapped by observing the motion of tracer particles either photographically or by Laser Doppler Anemometry. The most important result seems to be the observation of regions with strong secondary streaming at the inlet of the curved section, which, to the best of our knowledge, have not been reported before.

1. INTRODUCTION

Knowledge of the flow field in pipe bends with various inlet conditions is of importance both in engineering and physiology. U-shaped pipes of plexiglass has been used in this investigation in order to study such flow fields for purely oscillatory laminar inlet flow (i.e. the flow in the straight pipes far from the bend). The purpose was to map the flow field at various stations of the pipe and to interpret the results in the light of earlier theoretical and experimental investigations. In this context the papers of Lyne (1970 & 1971) and Mullin & Greated (1980) will be of special interest. The papers of Smith (1976) and Singh, Sinha & Aggarwal (1978) are also of some interest, but unfortunately these authors does not consider backflow of the axial components of the velocity.

The paper of Greated & Mullin is an experimental investigation of fully developed oscillatory laminar flow entering a curved pipe from a straight section. The investigation pays special attention to the alteration of the velocity profiles of the straight section to those of the curved pipe. We have also observed this alteration, but the main emphasis is put on non-linear streaming effects. Thus we have observed strong secondary flow at the inlet of the bend which to the best of our knowledge has not been reported before. The secondary streaming induced by oscillatory flow along a torous described theoretically by Lyne (1970), has also been observed.

The most convenient theoretical model with respect to comparison with some of our experimental data seems to be that of Lyne (1970) which describes the velocity field induced in a torous by a uniform axial pressure gradient varying sinousoidally in time.

For later use we quote some of his results here. Using perturbation methods it is possible to write the axial component of the velocity field induced by the aforementioned pressure gradient as the following asymptotic expansion,

$$(1) \qquad w = w_o(\eta,\tau) + \beta w_1(\eta,\tau) + \beta^2 w_2(\eta,\tau,R_s) + \delta w_{10}(\eta,\psi,\tau) + \delta\beta w_{11}(\eta,\psi,\ ) + \ldots$$

where w_o, w_1 and w_2 are given by equations (3.19), (3.36) and (3.50) in Lyne (1970), while Bertelsen (1974) using Lyne's expansion scheme found.

(2) $$w_{10} = -\left[\sin\tau - e^{-\eta}\sin(\tau-\eta)\right]\cos\psi$$

$$w_{11} = \eta\cos\psi\sin\tau$$

The parameters β and δ are assumed to be small and are defined as

(3) $$\beta = \frac{1}{a}\left(\frac{2\nu}{\omega}\right)^{\frac{1}{2}} << 1, \quad \delta = \frac{a}{A} << 1$$

where a is the radius of the pipe, ν the kinematic viscosity of the fluid, ω the circumferential frequency of oscillation and A the radius of the torous. The boundary layer coordinate η is defined as,

(4) $$\eta = (1-r)/\beta$$

where r is the dimensionless radial position $r = \bar{r}/a$ ($\bar{r}$ and ψ are radial and angular positions as indicated in figure 1).

The secondary steady streaming induced in the cross section plane of the pipe can be depicted by a stream function $\chi(r,\psi;\beta;R_s;\delta)$. Lyne (1970) gave an approximate solution of χ, where among other things, terms of order $O(\delta)$ were neglected. Including such terms, an uniformly valid expression of the stream function can be written,

$$(5)\quad \chi(r,\psi;\beta;R_s;\delta) = \beta X_o^{(s)}(\eta,\psi)+\beta^2 X_1^{(s)}(\eta,\psi)$$
$$+ \beta\delta X_{o1}^{(s)}(\eta,\psi) + \chi_{oo}(r,\psi)+R_s\chi_{o1}(r,\psi)$$
$$+ R_s^2\chi_{02}(r,\psi) + \beta R_s\chi_{11}(r,\psi)+\beta R_s^2\chi_{12}(r,\psi)$$
$$+ \beta^2\chi_{20}(r,\psi) + \beta^2 R_s\chi_{21}(r,\psi) + \delta\left[\chi_{oo1}(r,\psi)\right.$$
$$\left.+ \beta\chi_{101}(r,\psi) + R_s\chi_{011}(r,\psi)\right] - M(\eta,\psi;\beta;R_s;\delta)$$

where the functions involved, except for terms of order $O(\delta)$ and $M(\eta,\psi;\beta;R_s;\delta)$, are given explicitly by Lyne (1970) as follows: $X_o^{(s)}$ and $X_1^{(s)}$ are the steady parts of X_o and X_1 given by equations (3.26) p. 27 and (3.41) p.30, respectively; χ_{oo}, χ_{o1} and χ_{o2} are given by equations (4.4) p. 36, (4.6) p.37 and (4.8) p. 37, respectively; χ_{10}, χ_{11} and χ_{12} are given by equations (4.14), (4.16) and (4.18) p. 38, respectively; χ_{2o} and χ_{21} can be found from equation (4.20) p. 39 as,

$$(6)\quad \chi_2^{(s)} = \chi_{22} + R_s\chi_{21}$$

Bertelsen (1974) found

$$(7)\quad X_{01}^{(s)}(\eta,\psi) = \left[-\tfrac{5}{8} + \tfrac{1}{4}\eta + \tfrac{1}{8}e^{-2\eta} + \tfrac{e^{-\eta}}{2}(\sin\eta + \cos\eta)\right]\sin 2\psi$$

$$(8)\quad \chi_{oo1} = \tfrac{1}{8}(r^2-r^4)\sin 2\psi$$

$$(9)\quad \chi_{101} = -\tfrac{1}{16}(41\,r^2 - 31\,r^4)\sin 2\psi$$

$$(10)\quad \chi_{011} = \tfrac{1}{18432}(8r - 33\,r^3 + 42\,r^5 - 17\,r^7)\sin\psi$$
$$+ \tfrac{67}{61440}(r^3 - 2\,r^5 + r^7)\sin 3\psi$$

$$(11)\quad M = \beta(\tfrac{5}{8} - \tfrac{1}{4}\eta)\sin\psi + \beta^2(-\tfrac{3}{16} + \tfrac{1}{2}\eta)\sin\psi$$
$$+ \beta^2(\tfrac{3}{8}\sin\psi - \tfrac{Rs}{768}\sin 2\psi + \tfrac{Rs^2}{737280}\sin\psi)\eta^2$$
$$+ \beta\delta(-\tfrac{5}{8} + \tfrac{1}{4}\eta)\sin 2\psi$$

The stream function given by equation (5) above will serve the basis of comparison with measured velocities in the middle cross section plane of the bend (i.e. cross section 1 in figure 2). The time averaged velocity $(\bar{u},\bar{v})$ in this cross section is given by (physical dimensions),

$$(\bar{u},\bar{v}) = \varepsilon^2\omega a\left(\frac{1}{r}\frac{\partial \chi}{\partial \psi}, -\frac{\partial \chi}{\partial r}\right) .$$

2. THE EXPERIMENTAL SYSTEM

2.1 The pipesystem and the pumps

The esperiments described in this paper were performed in a pipe system of plexiglass. The system consisted of a bend (180^{o}) connected to two straight pipes by smooth junctures (A & B in figure 2). The bend is cut as a circular channel through a plexiglass block by a milling machine. Two models have been used, model I with $\delta = 1/6$ and model II with $\delta = 1/4$. Two pumps were connected to straight pipes (see figure 2) and forced the fluid to oscillate with a frequency stability of approximately 1 %. The amplitude of the overharmonics of the motion of the pistons were 2% or less relative to the amplitude of the basic frequency. A disk with a hole was fixed on the shaft of the pump. An electrooptical device (Texas Instruments, TIL 138) was so mounted relative to the disk that the light path was open just when the hole passed the device. A pulse train is therefore generated when the disk rotates. This pulse train was used to obtain phase locked sampling of the velocity field in the pipe.

2.2 Method of observation and data acquisition.

The velocity field induced in the pipe system by the oscillating pistons were observed to some extent by photographic recording, but mainly by using a commercial available Laser Doppler anemometer (LDA), DISA 55 L, Mark II. Titanium oxide was added to the fluid in order to obtain sufficient scattered light for the LDA-measurements. The optical components including the laser and the photomultiplier were mounted on a three axis coordinate system which could be moved to any position within its range and resolution by driving three step motors. Changes of position were controlled by a HP 9825A desk computer which also served the duty as controller of a HP3052A Data Acquisition System equipped with the following main components: A scanner HP3495A, a multimeter HP3455A and a system voltmeter HP3437A. The multimeter was used to read the position indicators (potentiometers) while the system voltmeter sampled the output of the LDA. In order to measure the instantaneous

velocity distribution across the pipe it was necessary to sample the velocity phase locked relative to the pumps. This was achieved utilizing the external triggering facility of the system voltmeter. The pulsetrain generated by the electrooptical device mentioned above, passed some pulse-shaping electronics before it was fed to the "external triggering" input of the system voltmeter. The controller was programmed to let the external trigger initiate a sequence of typically ten samples during one period of the oscillatory motion of the fluid before the next external trigger pulse initiated a new sequence. The delay between each measurement in a sequence was controlled by the system voltmeter's own clock and was chosen to give the time interval between the last measurement in a sequence and the first in the next sequence to be equal the delay itself. In this way several sequences gave a series of measurements all equally spaced in time. The velocity and position readings and other data of interest were fed to the controller and stored on magnetic tape.

The purpose of the photographic recording, mentioned above, was two fold. The recordings gave information of the gross features of the secondary streaming (see figure 11). A second aim was to check the readings of the LDA as far as the secondary steady streaming is concerned. The fluid layers which were photographed, were illuminated by a sheet of stroboscopic light with a repetition frequency equal to the frequency of the pumps. Aluminium powder was added to the fluid to render the motion visible.

2.3 Data analysis and validation tests

The velocity readings collected as described above, was analysed using a FFT-routine supplied by Hewlett Packard. The analysis proceeded as follows: Each sequence, say j, consisting of typically ten samples taken in one period of the oscillatory motion of the fluid, was analysed by the FFT-routine giving the Fourier coefficients,

$a_{o,j}$, $a_{1,j}$, $a_{2,j}$ (cosine terms)

$b_{1,j}$, $b_{2,j}$ (sine terms)

A sufficient number of sequences (N) was used to get the standard deviations

$$\Delta a_i = \sqrt{\frac{1}{N-1} \sum_{j=1}^{N} (a_{i,j} - a_i)^2} \quad , \quad i = 0,1,2 \tag{12}$$

$$\Delta b_i = \sqrt{\frac{1}{N-1} \sum_{j=1}^{N} (b_{i,j} - b_i)^2} \quad , \quad i = 1,2 \tag{13}$$

of the mean values

$$a_i = \frac{1}{N} \sum_{j=1}^{N} a_{i,j} \tag{14}$$

$$b_i = \frac{1}{N} \sum_{j=1}^{N} b_{i,j} \tag{15}$$

below some chosen limits. The phase of the basic frequency was determined by putting

$$a_1 \cos \tau + b_1 \sin \tau = \sqrt{a_1^2 + b_1^2} \sin (\tau + \phi) \tag{16}$$

giving

$$\varphi = \arccos\left(\frac{b_1}{\sqrt{a_1^2 + b_1^2}}\right) \tag{17}$$

2.4 The working fluid

In order to obtain LDA-measurements close to the pipe walls and to have non-disturbed photographic recordings from these regions, it was necessary to use a fluid with the same index of refraction as the plexiglass. A mixture of approximately 74 % kerosine (Shellsol K) and 26 % (by volume) of a lubricating oil (Gravex 19, Shell) had this property. The refraction indices of the fluid and the plexiglass were matched within 1‰. The kinematic viscosity of the fluid was approximately 0.16 cm^2/s at 283°K and the temperature coefficient was 0.0086 $cm^2/s°K$.

3. RESULTS AND DISCUSSION

Measured velocities in five cross sections around the pipe system will be presented here. The cross sections were located as indicated in the following table where s is the distance from the juncture of the bend and the straight pipe to th cross section in question (the distance being measured along the axis of the pipe and reckoned positive into the straight section, see figure 2).

Table 1

Model	Cross section:	Distance s (mm)				
		1	2	3	4	5
Model I		-94.25	-3.95	-1.64	1.32	42.11
Model II		-62.83	-2.04	-0.72	1.91	42.70

3.1 The inlet flow conditions

On the basis of the construction of the pumps, we could not expect pure simple harmonic motion of the fluid in the straight section of the pipe. Therefore the inlet flow conditions were investigated experimentally by measuring the time evolution of the axial velocity component in cross section 5 (r=o) during several hundred periods of the pistons motion. The measured velocities are plotted in figure 4 where also a simple harmonic motion is indicated. The experimental values are average values of the velocity measured at a fixed phase in each period. The figure indicates that the inlet flow is sufficient close to simple harmonic motion that it will make sense to attribute expected non linear effects in the bend to selfinteraction of the motion with the basic frequency.

The axial velocity profile along a diameter in cross section 5 has been investigated experimentally. On the basis of these measurements the phase-variation along the diameter was calculated. The results are plotted in figure 5 where also a theoretical curve based on equation 1 with $\delta=R_s=0$ is indicated. The theoretical curve is known to be a good approximatin to the real phase varia-

tion. Therefore we interpret the results presented in figure 5 to imply that the method of observation, including the phase locked sampling of the LDA output, worked satisfactorily.

3.2 The axial time dependent component of the velocity

The axial component of the velocity field was measured at 5 cross sections along the pipe. Figure 6 and 7 show the measured values against radial position in model I and II. There is (to our knowledge) no theoretical model which describes the alteration of the velocity profiles in a straight pipe to those in the bend. Therefore, theoretical profiles for a straight pipe and torous based on equation (1) (in the straight pipe $R_s=\delta=0$), only, could be drawn in the aforementioned figures. The amplitude of theoretical and measured values of the velocity was put equal at r=0. The measured values are the amplitudes ($\sqrt{a_1^2 + b_1^2}$ in equation 16) of the basic frequency. On the basis of figure 6 and 7 we conclude that the change of the velocity profile in the straight pipe to those of the bend take place over a typical length equal to a (the radius of the pipe). This is also expected on the basis of "order-of-magnitude" arguments. The length scale is expected to be determined by the potential flow outside the Stokes layer. The governing length scale in the potential flow around a body is usually a characteristic dimension of the body, in this case the radius of the pipe. This differs from the results of Mullin & Greated 1980 which showed fully developed torous flow at $s \approx -A$. In their experiments, however, the β-values were, $0.2 \lesssim \beta \lesssim 1$. For such β-values the viscosity is important in the core of pipe also. Therefore the results discussed above are not contradictory.

The first harmonic of the basic frequency was also attempted measured. However, it turned out to be very difficult to get the error bounds of a_2 and b_2 sufficiently small to obtain meaningful results. (These problems could be due to elasticity

and photoelasticity in the plexiglas models.) Therefore, no measurements of a_2 and b_2 are discussed here.

3.3 The steady secondary streaming

Measurement of the steady secondary streaming is difficult in our case because it is heavily modulated by a large amplitude oscillatory flow. In order to test our method of observation, we measured the secondary streaming in cross section 1. In this region of the bend we expect Lyne's model added some terms due to finite aspect ratio δ and given by equatin 5, to be a good approximation to the real flow field.*) This theoretical model is compared to measured velocities in figure 8, 9 and 10. We think the good agreement between theoretical and measured velocities in this figure imply that the method of observation worked satisfactorily, also with respect to reveal secondary flows. Other regions in the pipe system susceptible to non linear streaming effects, are the regions around the junctures of the straight pipes and the bend. The gross features of the secondary streaming in these regions are shown in figure 11 which is drawn on the basis of several photographs of a fluid layer in the axial plane of the U-shaped pipe. Such photographs together with direct visual observation indicate that there is a Stokes layer at the walls where the Reynolds stresses induce a steady velocity which then by viscous action force the fluid in the core of the pipe to recirculate in an "egg-formed" region. More detailed information of this secondary streaming is given in figures 12, 13 and 14 where the axial component of the secondary streaming at different cross sections are plotted. There appears to be no essential difference between figure 12 and 13 where data from model I and II, both with frequency f=12 Hz, are presented. The maximum streaming velocity seems to be a little higher in figure 13. This difference is expected since the generating mechanism of the secondary streaming probably is the time averaged Reynolds stresses

$\rho \overline{w_o \frac{\partial w}{\partial s}}$ where $dw \sim O(\delta w_o)$ (w_o amplitude of basic flow). The same

*) Presupposed $R_s < 30$.

is true for figure 14 where f=9 Hz.

In figures 15 and 16 measured values of the radial component of the secondary flow at cross secion 4 are presented. These figures too indicate that the main features of the secondary streaming (except for the amplitude) are weakly dependent on the frequency when $\beta \ll 1$. The most striking feature of figure 15 and 16 is the change of sign of radial velocity when δ decreases from 1/4 to 1/6. This effect can most easily be observed in the streamline diagram of figure 11 from which it is easily seen that the core of the recirculating region is being displaced due to finite δ-values.

4. CONCLUSIONS

An important conclusion which can be drawn from the results presented here is that essentially fully developed oscillating flow in a straight pipe and in a bend apply at positions of order O(a) from the juncture of two such pipe components, presupposed the Stokes layer is thin compared to the radius of the pipe. On the other hand, if the Stokes layer thickness is of the order of the pipe radius, then the results of Greated & Mullin (1980) should apply. They found fully developed flow in the bend at positions of order O(A) from the inlet. The theoretical investigations of Smith (1976) and Singh al. (1978) do not allow backflow, but to the extent that any comparison with these results can be done, they are in accordance with our experiments. For example Smith (1976) found both an upstream and a downstream inlet effect in a pipe model as that used here.

Finally, the most important result is probably the demonstration of the secondary streaming in the region at the juncture of the straight pipe and the bend. A corresponding non-linear effect will probably persist in a pulsating (non zero mean) basic flow, but this problem is left for later investigations.

From an experimental point of view it is of some interest that it was possible to detect secondary flow around the inlet of the bend where this flow is heavily modulated by the basic flow. The error bounds of the LDA-measurements are large, but they can probably be improved by more sophisticated sampling techniques and more patience of the experimentalist.

List of references.

Bertelsen, A. F. 1974 Department of Physics, University of Bergen, Norway, Report No. 67

Lyne, W. H. 1970 Ph. D. Thesis University of London

Lyne, W. H. 1971 J. Fluid Mech. 45, 13 - 31

Mullin, T. & Greated, C. A. 1980 J. Fluid Mech. 98, 383 - 396

Singh, M. P., Sinha, P. C. & Aggarwal, M. 1978 J. Fluid Mech. 87, 97 - 120

Smith, F. T. 1976 Proc. R. Soc. Lond. A, 351, 71 - 87

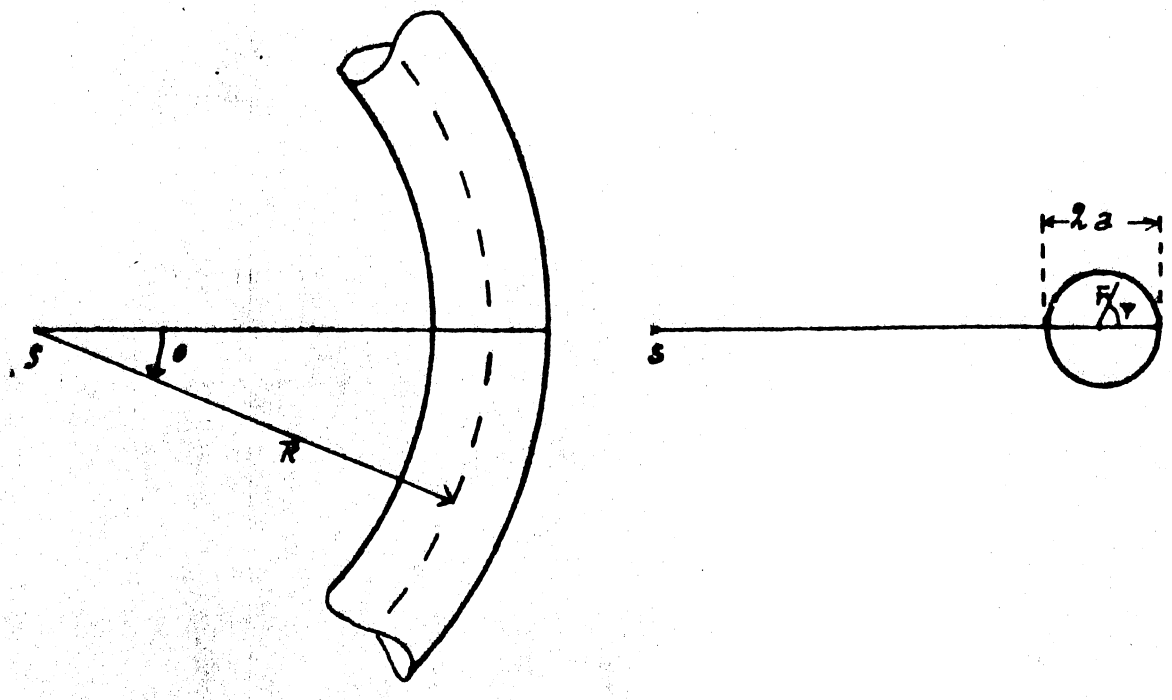

Figure 1. The coordinate system referred to in the text.

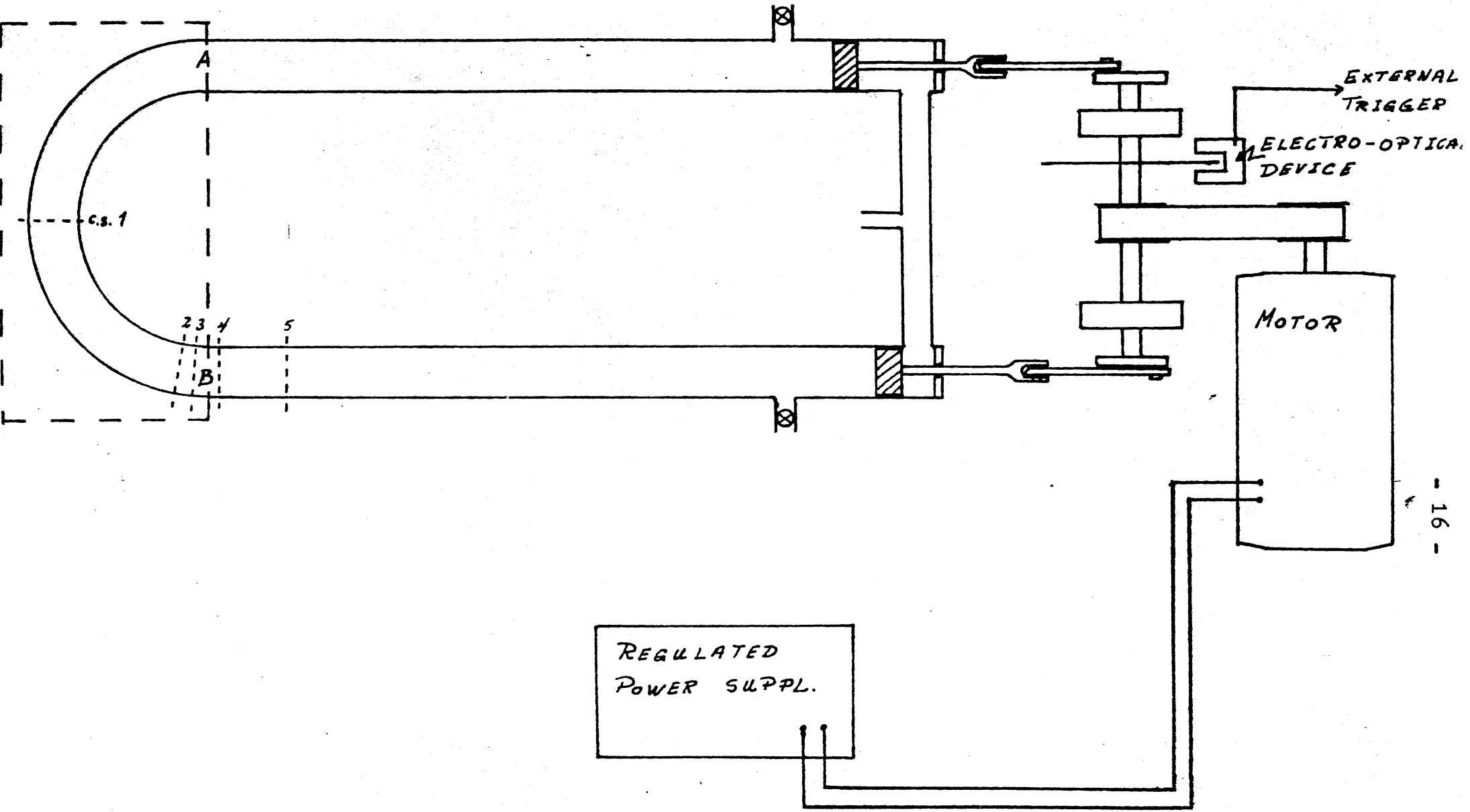

Figure 2. The figure shows the main components of the pipe system and the pump. The cross sections where measurements are performed are indicated (c.s. 1, 2, 3, 4 & 5).

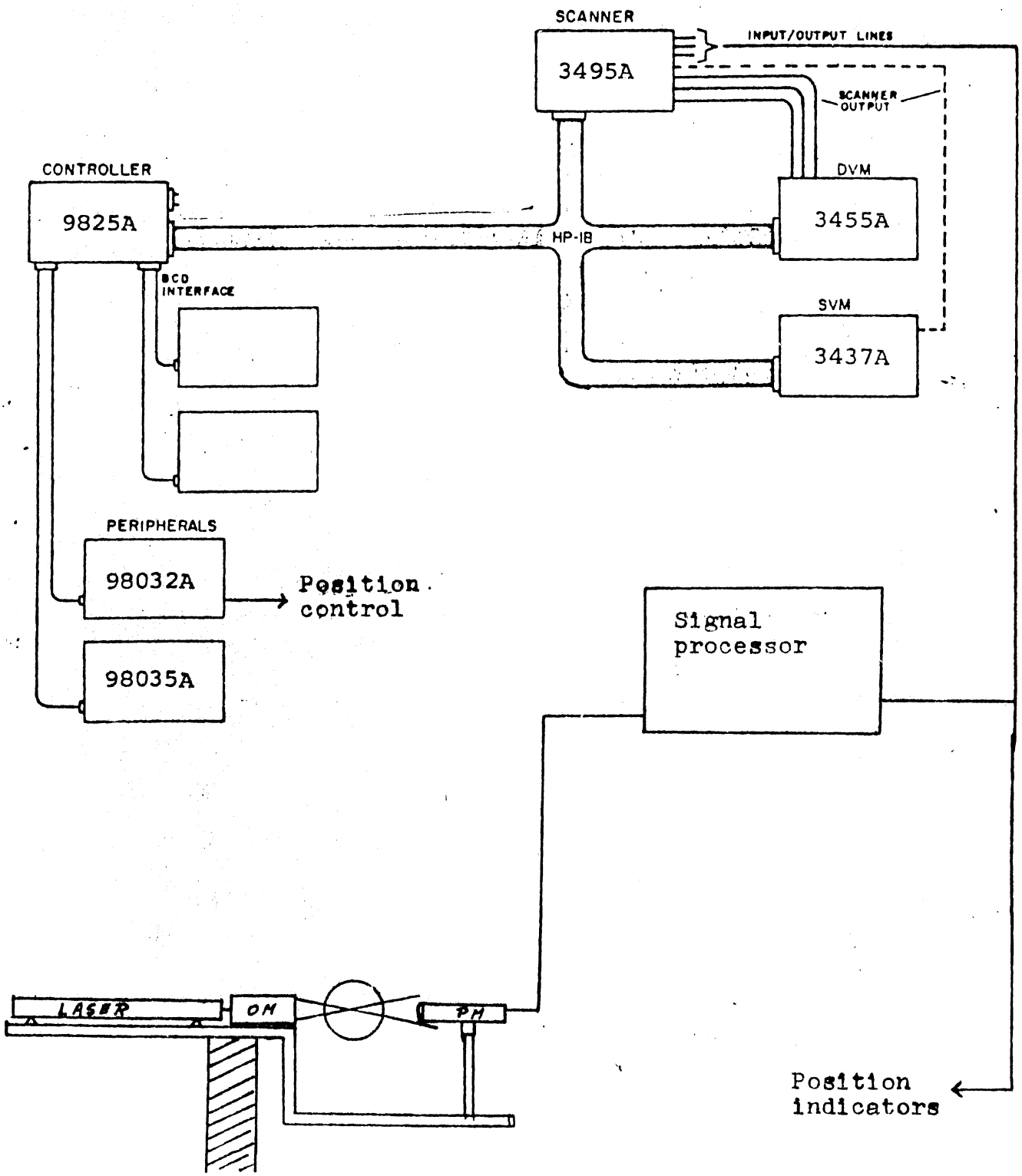

Figure 3. The figure show the main components of the Laser Doppler Anemometer and the data acquisition system. OM and PM indicate optical modulator and photomultiplier, respectively.

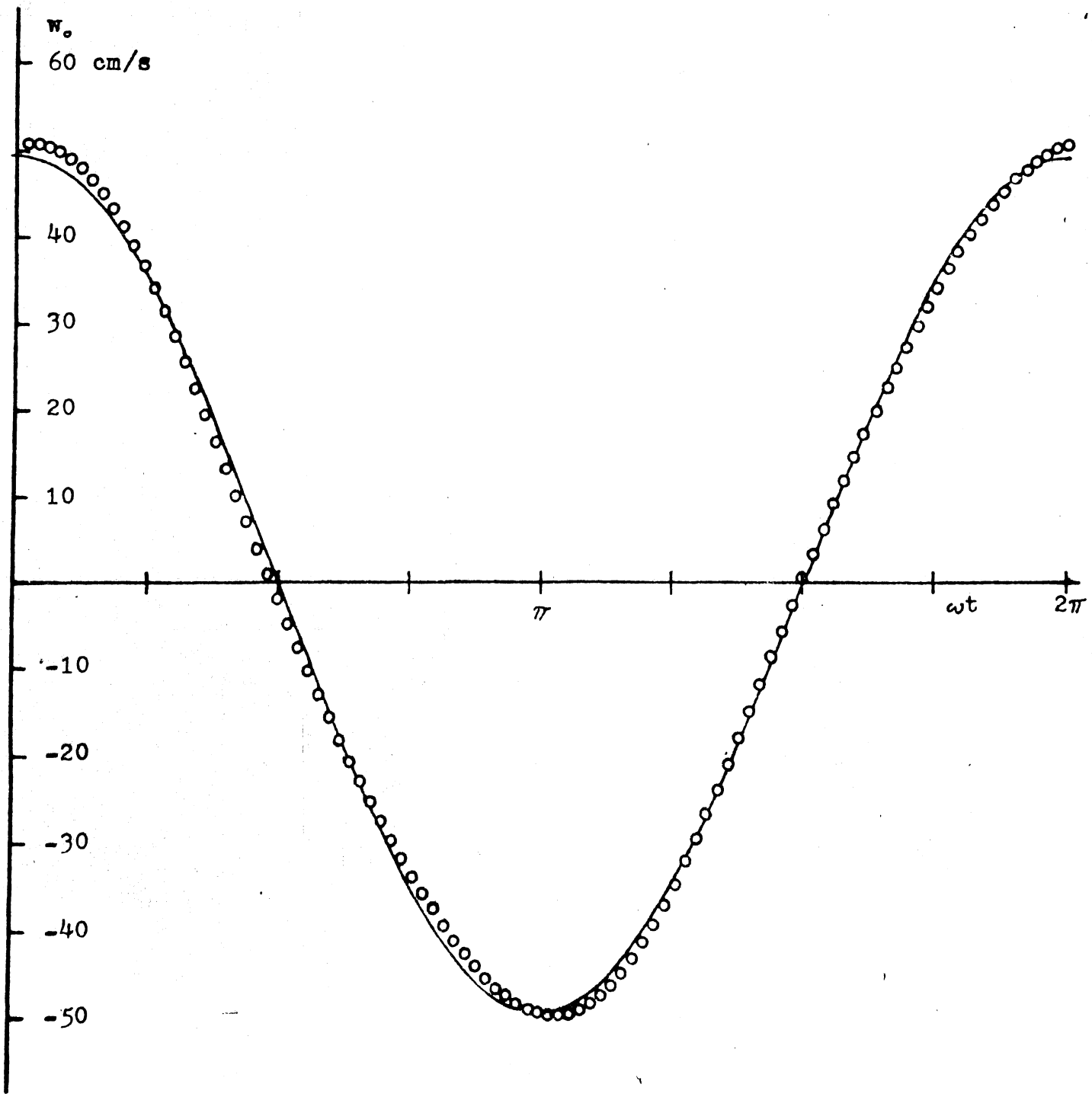

Figure 4. The basic flow, w_o , at cross section 5 (r = 0) as function of time. Continuous curve is simple harmonic motion with frequency 12 Hz, circles indicate measured values.

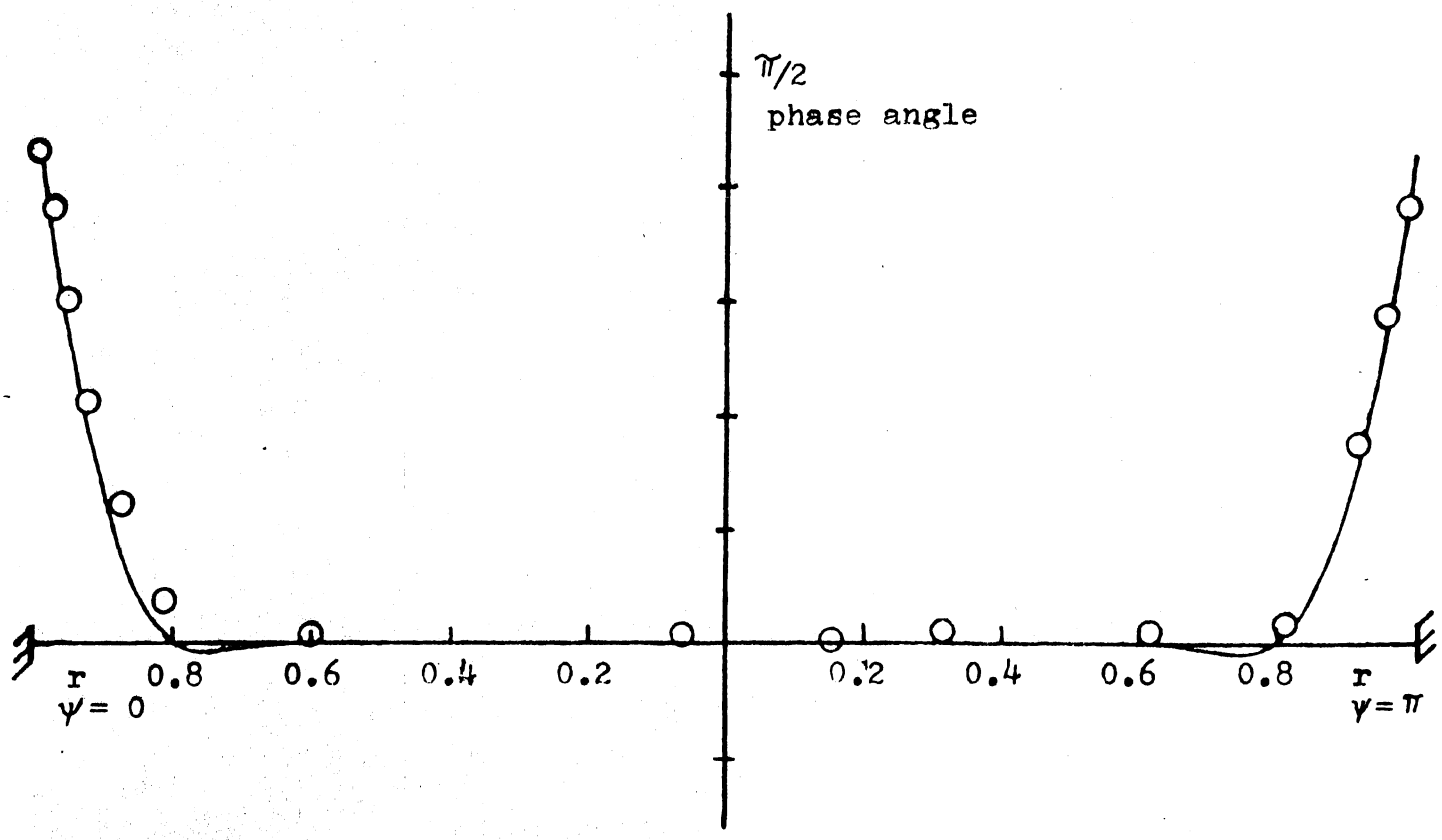

Figure 5. The phase-variation along a diameter. The continuous curve is based on equation 1 ($\sigma = R_g = 0$), circles indicate measured values.

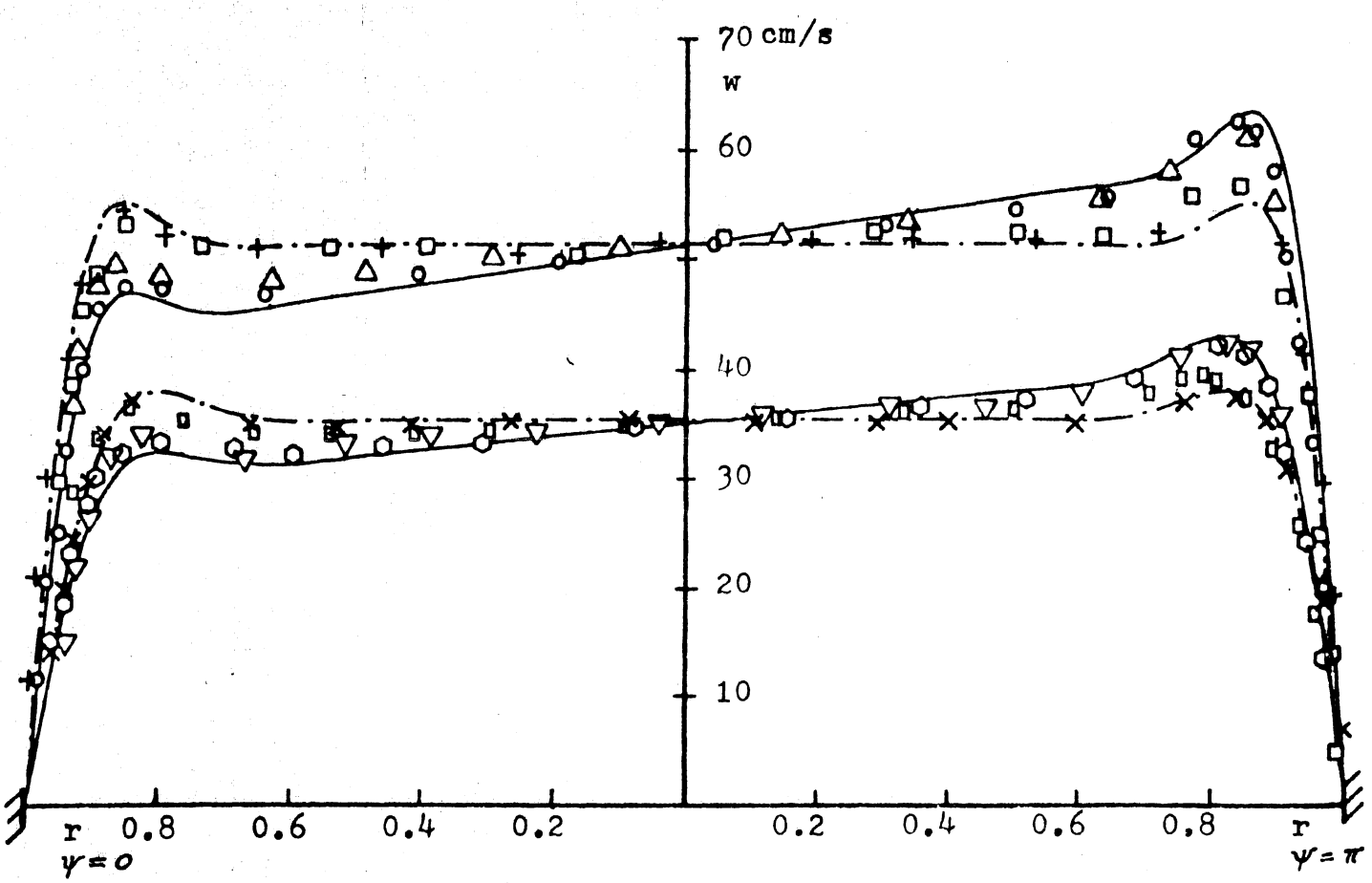

Figure 6. The profile of the unsteady, axial component of the velocity along a diameter in model I. The curves are based on equation 1: The upper continuos curve; f = 12Hz, β = 0.063, δ = 1/6, R_s =39.0. The lower continuous curve; f = 9Hz, β = 0.080, δ = 1/6, R_s = 20.4. The corresponding broken curves have the same parameter values except for $\delta = R_s = 0$. The corresponding measured velocities at some points are also plotted. o, Δ, □ and + indicate measurements for f = 12Hz in cross sections 2, 3, 4 and 5, respectively. ○, ▽, ▯, and × indicate measurements for f = 9Hz in cross sections 2, 3, 4 and 5, respectively.

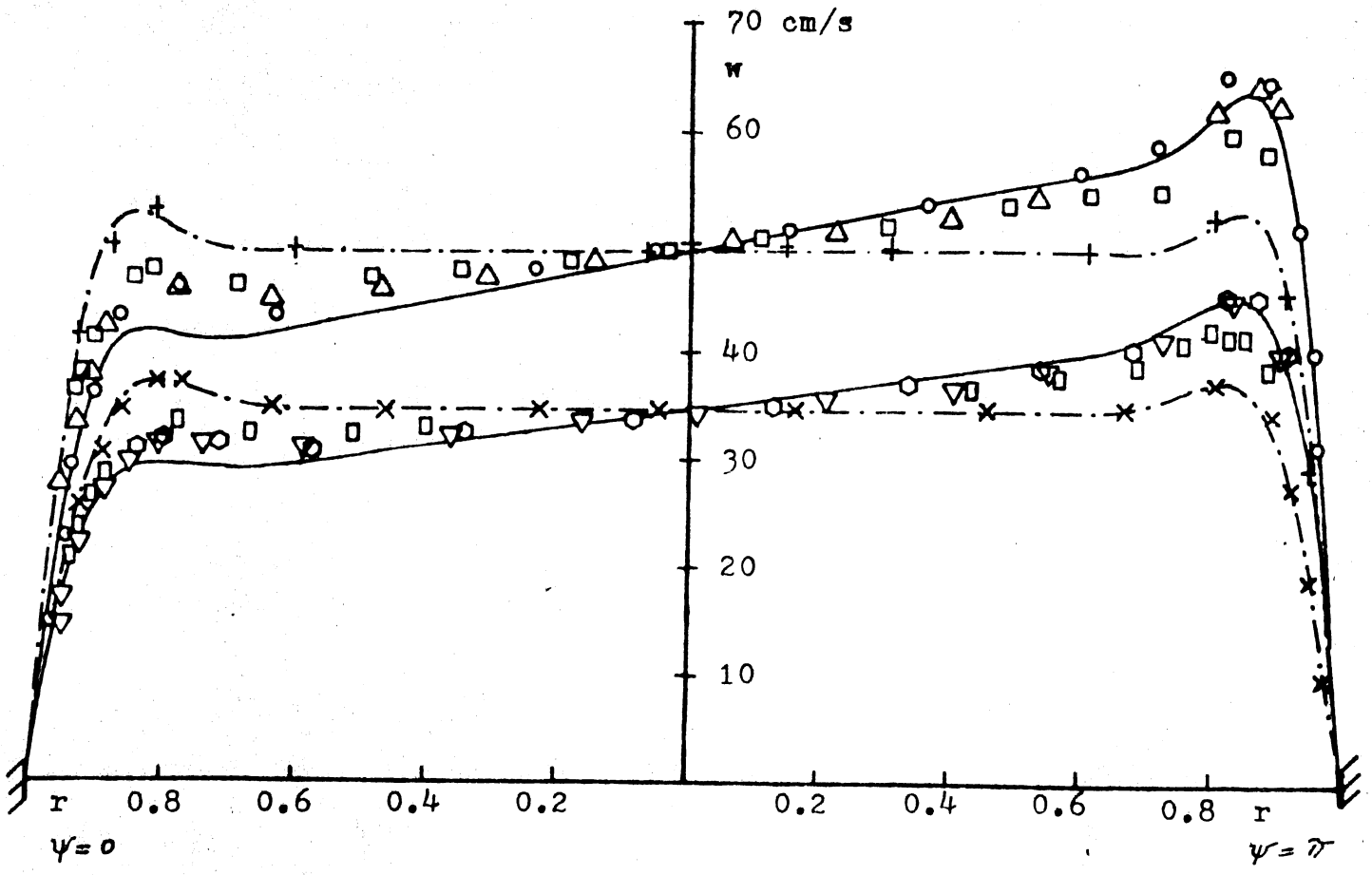

Figure 7. The profile of the unsteady, axial component of the velocity along a diameter in model II. The curves are based on equation 1: The upper continuous curve; f = 12Hz, β = 0.065, δ = 1/4, R_s = 50.0. The lower continuous curve; f = 9Hz, β = 0.079, δ = 1/4, R_s = 29.8. The corresponding broken curves have the same parameter values, except for $\delta = R_s = 0$. The measured velocities at some points are also plotted. o, □, Δ and + indicate measurements for f = 12Hz in cross sections 2, 3, 4 and 5, respectively. o, ▽, ▯ and × indicate measurements for f = 9Hz in cross sections 2, 3, 4 and 5, respectively.

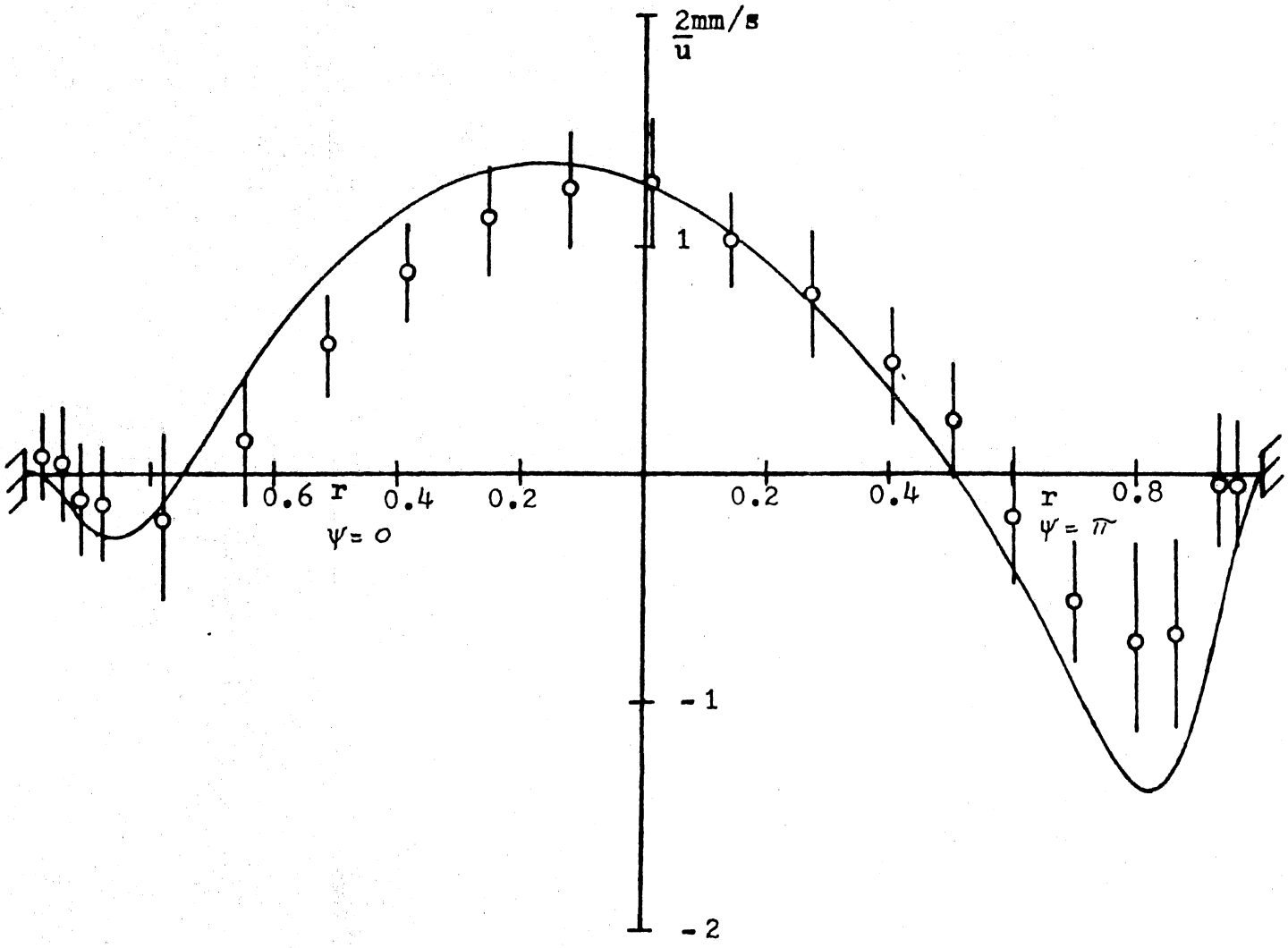

Figure 8. The time averaged radial velocity $\bar{u}$ along a diameter in cross section 1 in model I. The parameters have the same values as given for the measurements with 9Hz in figure 6. The continuous curve is based on equation 5. ϕ indicate LDA measurements. The velocity is reckoned positive towards the center of curvature of the bend.

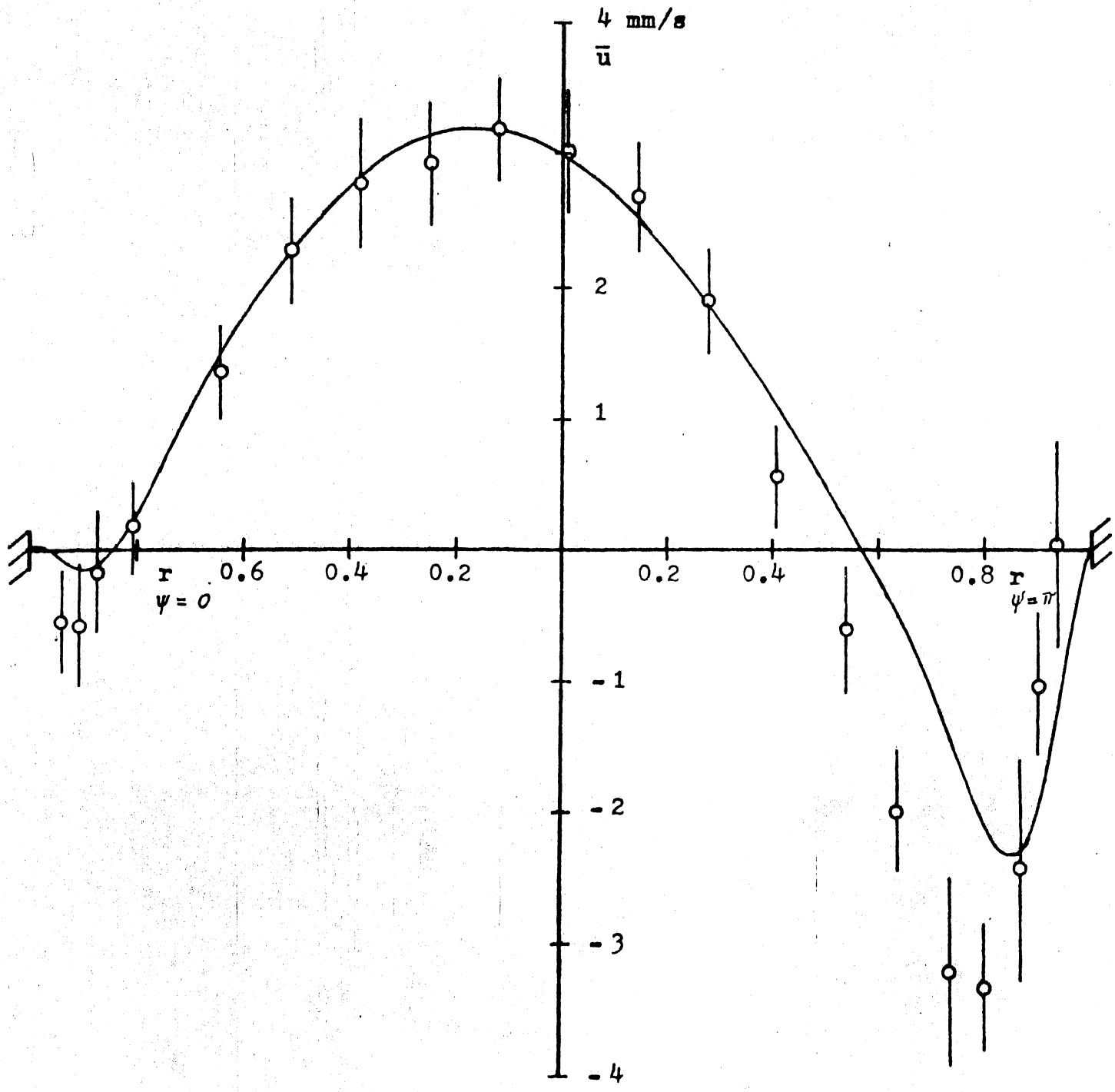

Figure 9. The time averaged radial velocity $\bar{u}$ along a diameter in cross section 1 in model II. The parameters have the same values as given for the measurements with 12Hz in figure 7. The continuous curve is based on equation 5. ϕ indicate LDA measurements.

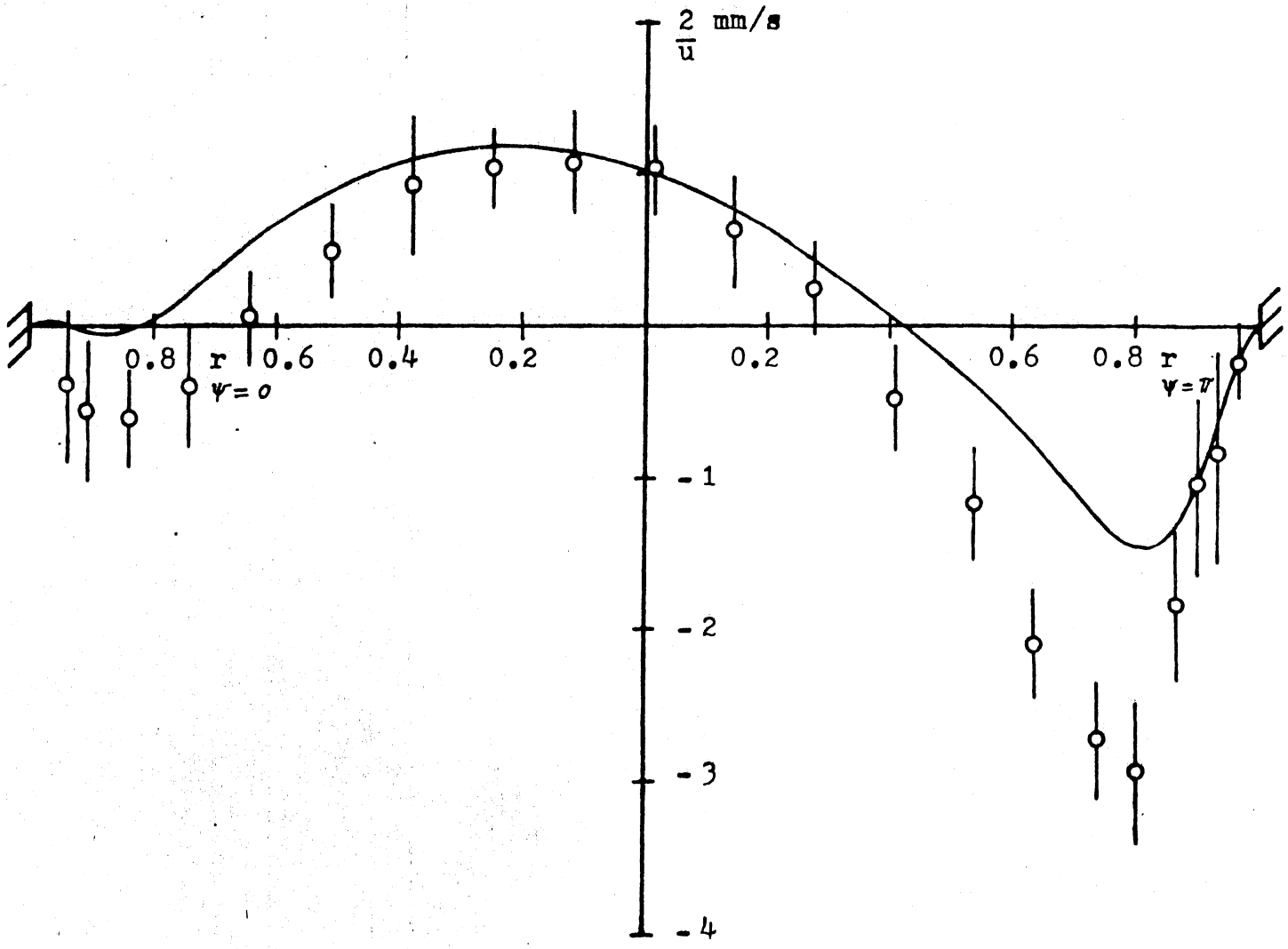

Figure 10. The time averaged radial velocity $\bar{u}$ along a diameter in cross section 1 in model II. The parameters have the same values as given for the measurements with 9Hz in figure 7. The continuous curve is based on equation 5. ϕ indicate LDA measurements.

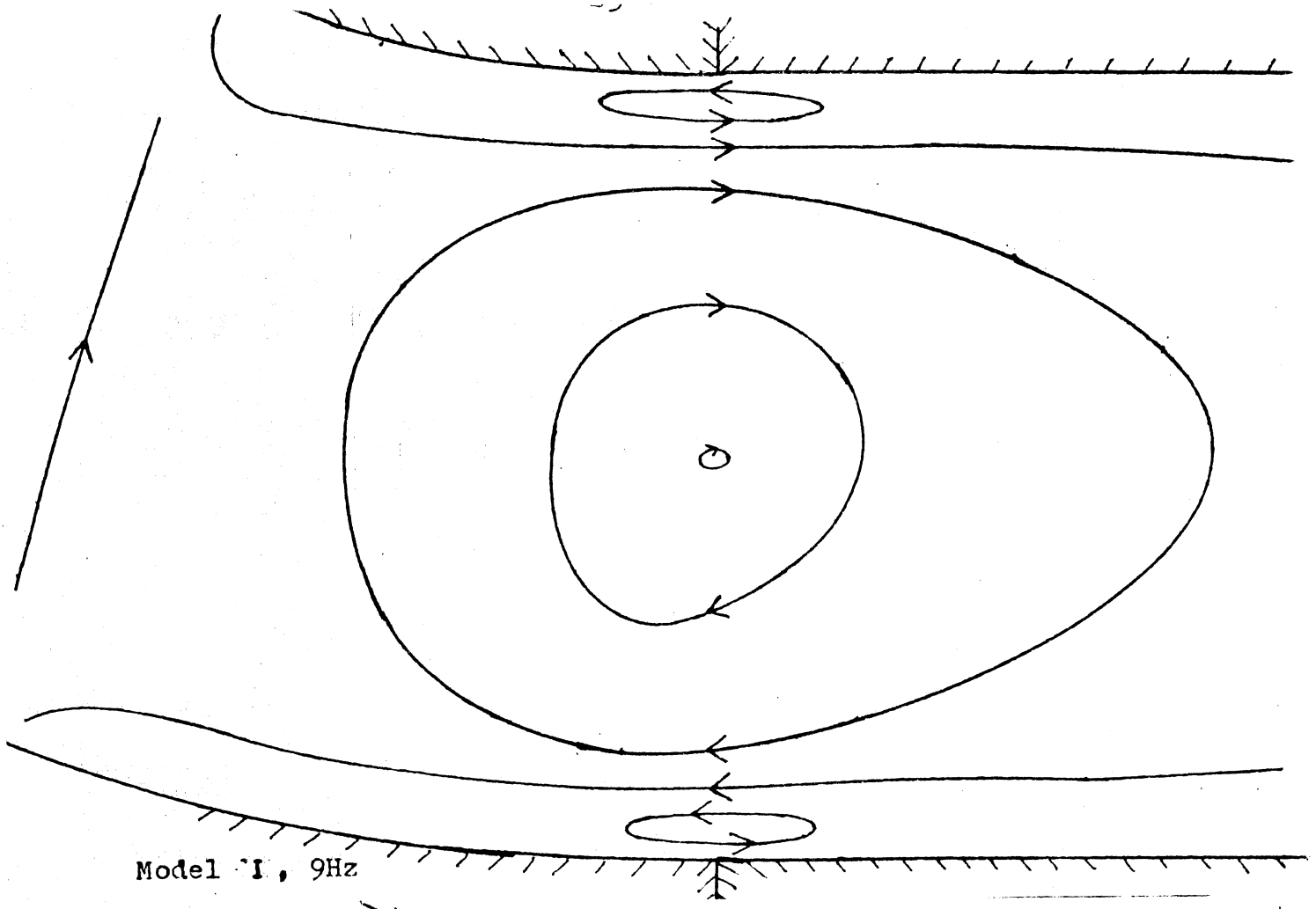

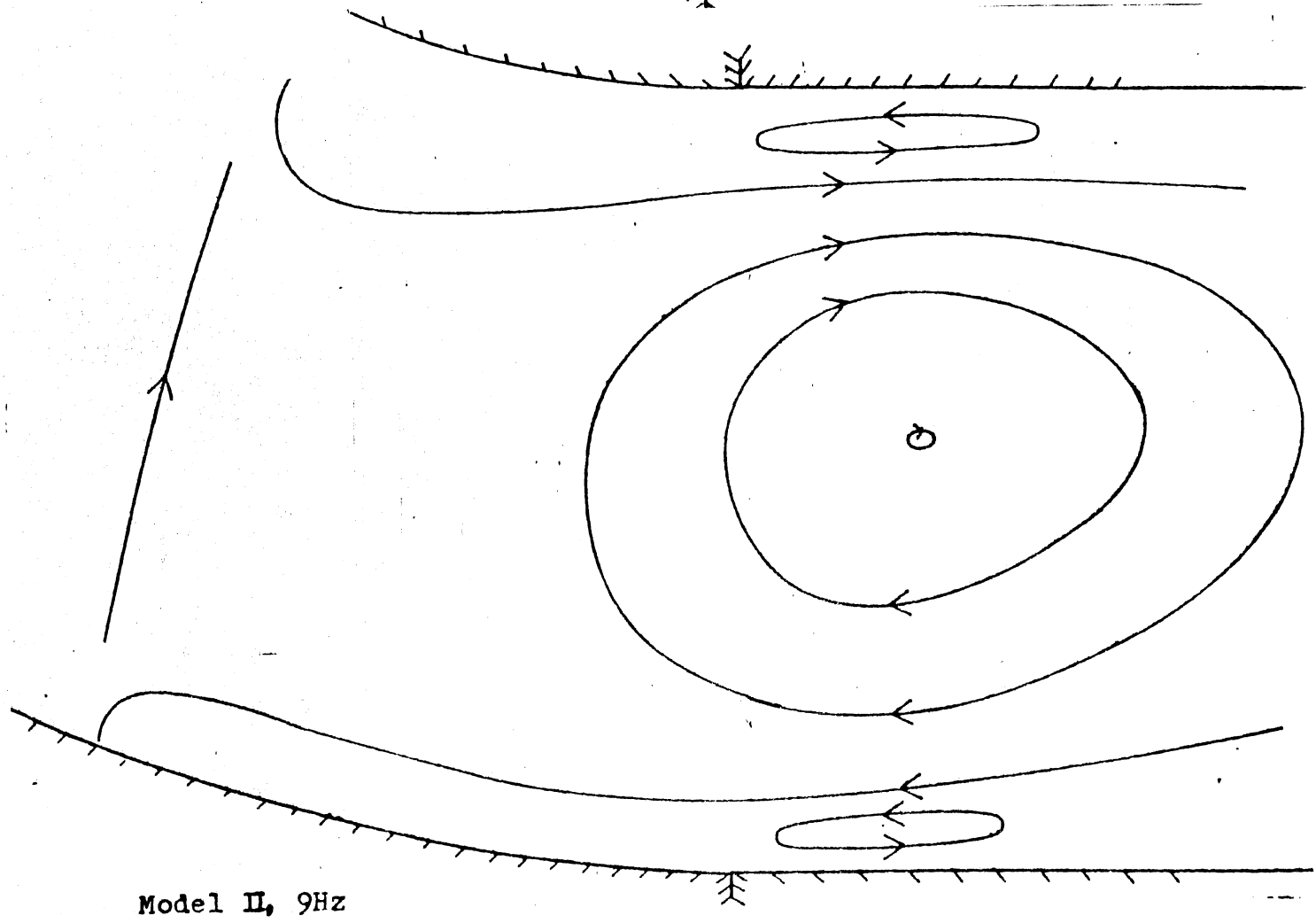

Figure 11. The main features of the secondary flow in the axial plane at the juncture of the straight pipe and the bend.

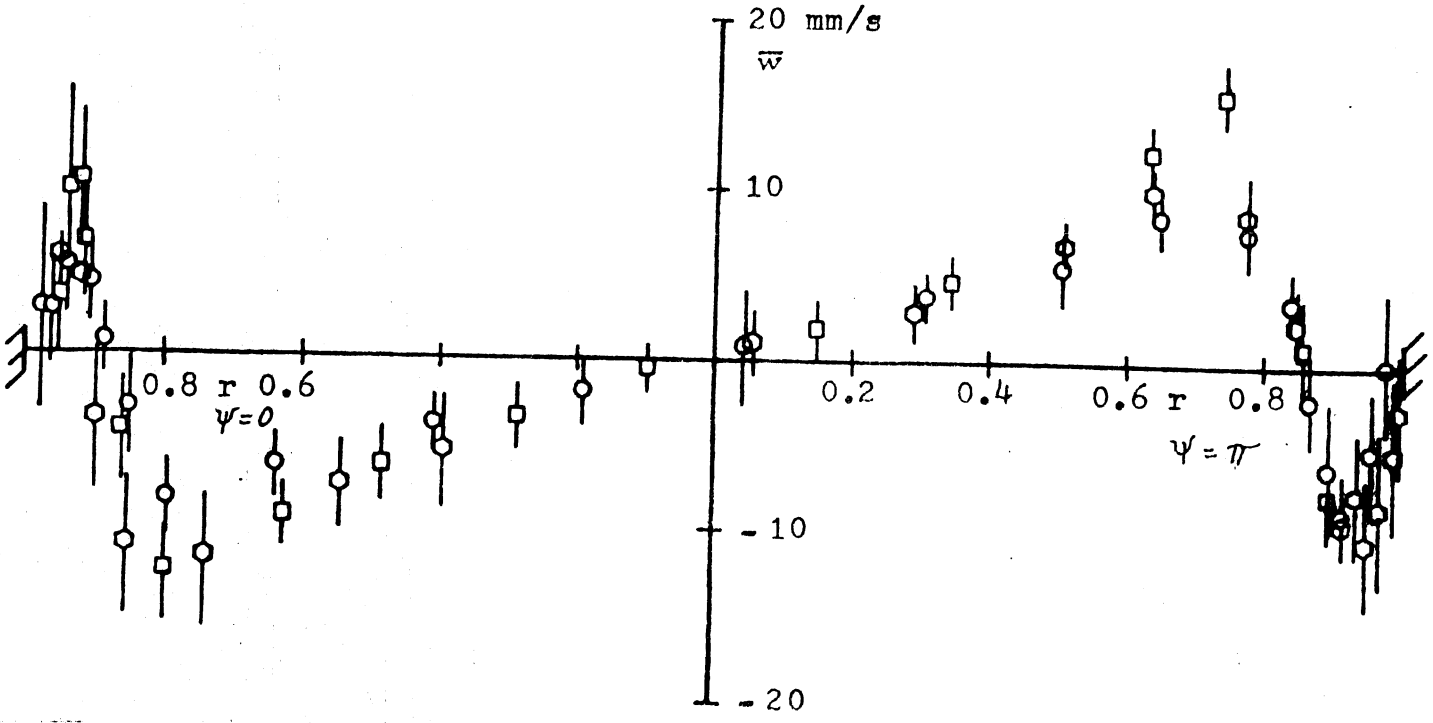

Figure 12. The measured time averaged axial velocity component $\bar{w}$ in model I with frequency f= 12Hz (other parameters, see figure 6). ○ , ◻ and ◇ indicate LDA measurements in cross sections 2, 3 and 4, respectively.

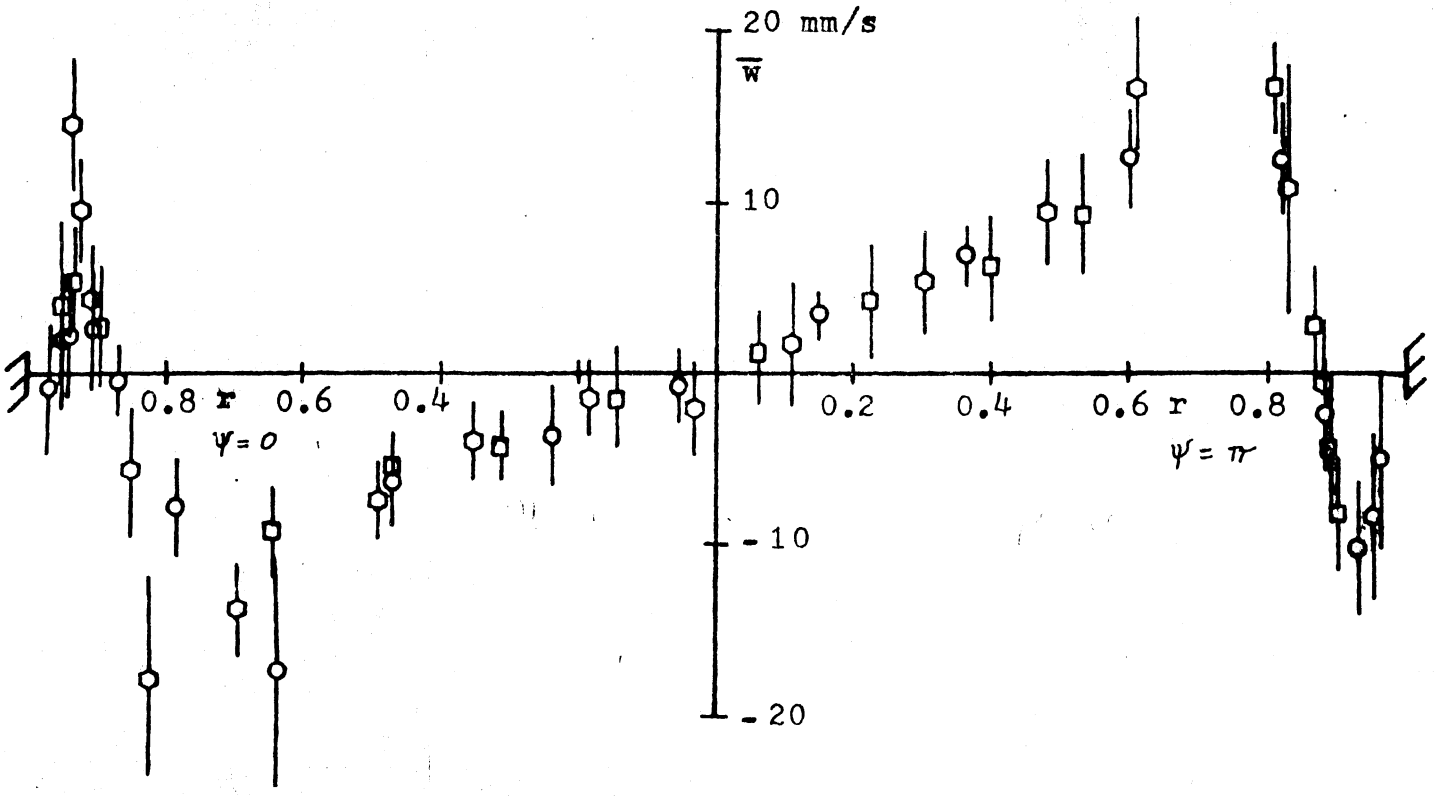

Figure 13. The measured time averaged axial velocity component $\overline{w}$ in model II with frequency f = 12Hz (other parameters, see figure 7). ϕ, ϕ and ϕ indicate LDA measurements in cross sections 2, 3 and 4, respectively.

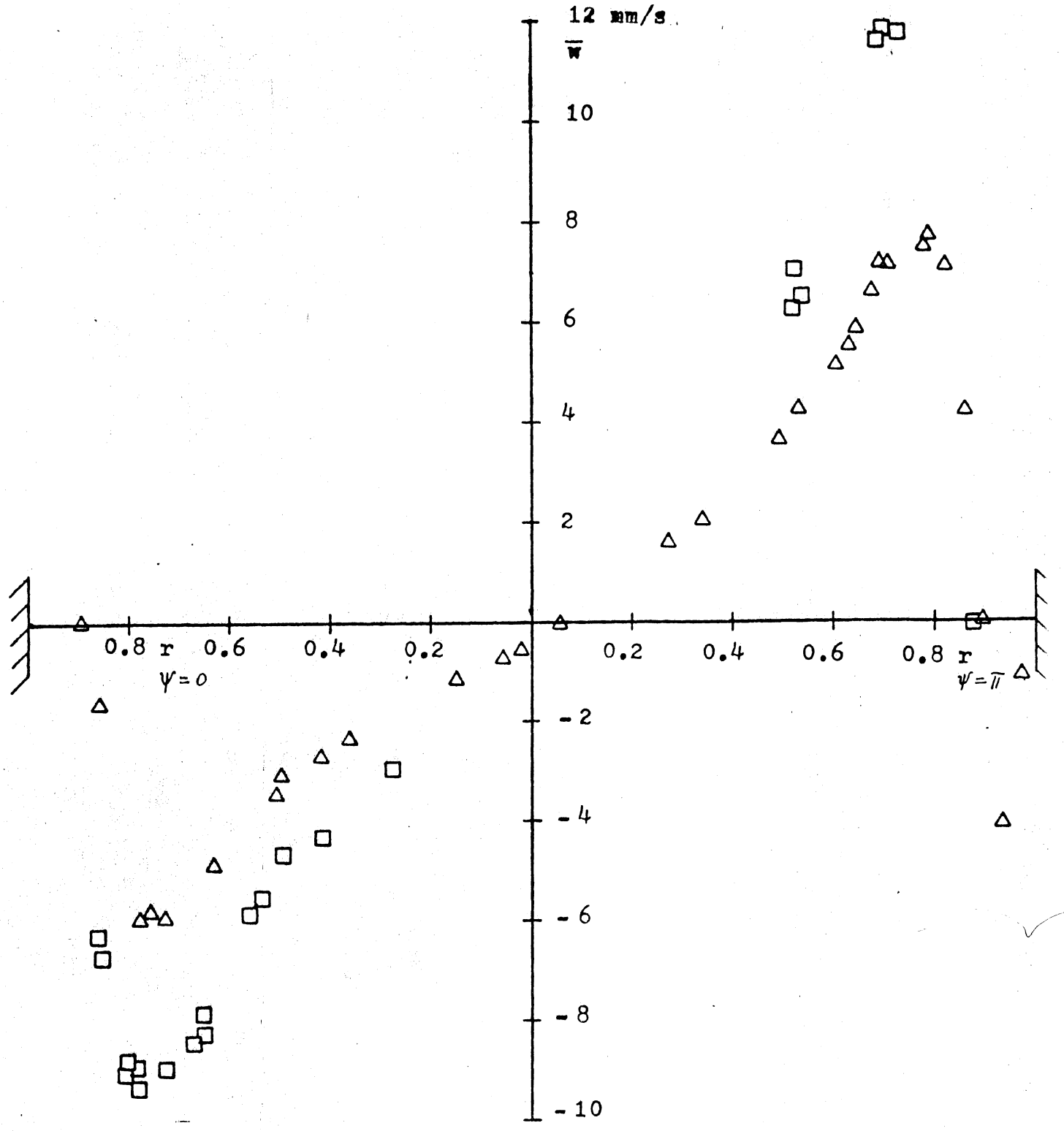

Figure 14. The measured time averaged axial velocity component $\overline{w}$ in model I and II, both with frequency f = 9Hz and in cross section 4 (other parameters, see figures 6 and 7, respectively). and indicate measurements in model I and II, respectively, based on photografic recordings.

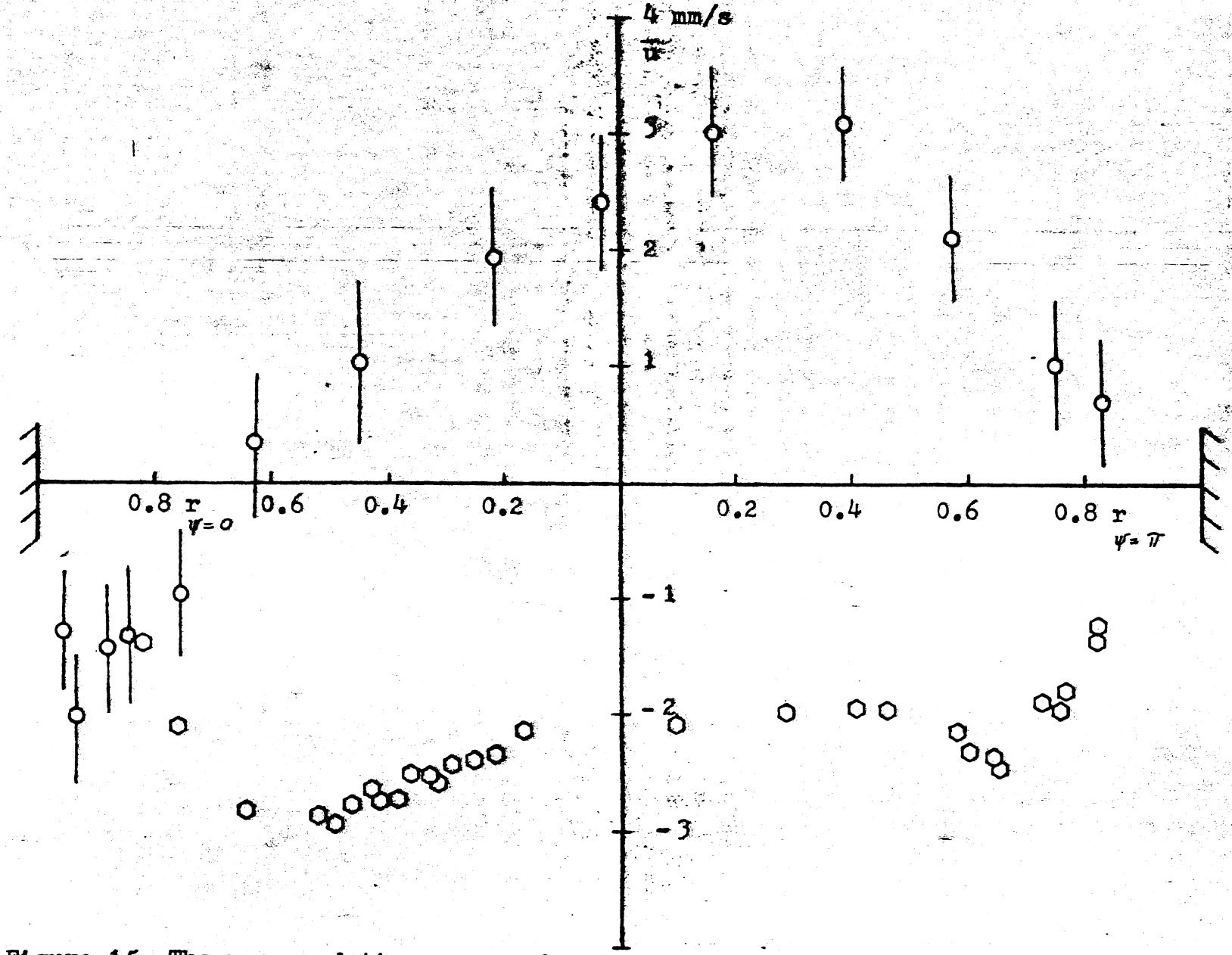

Figure 15. The measured time averaged radial velocity component $\bar{u}$ in model I and II, both with frequency f = 12Hz and in cross section 4 (other parameters, see figures 6 and 7, respectively) O and ϕ indicate measurements in model I (photo) and II (LDA), respectively.

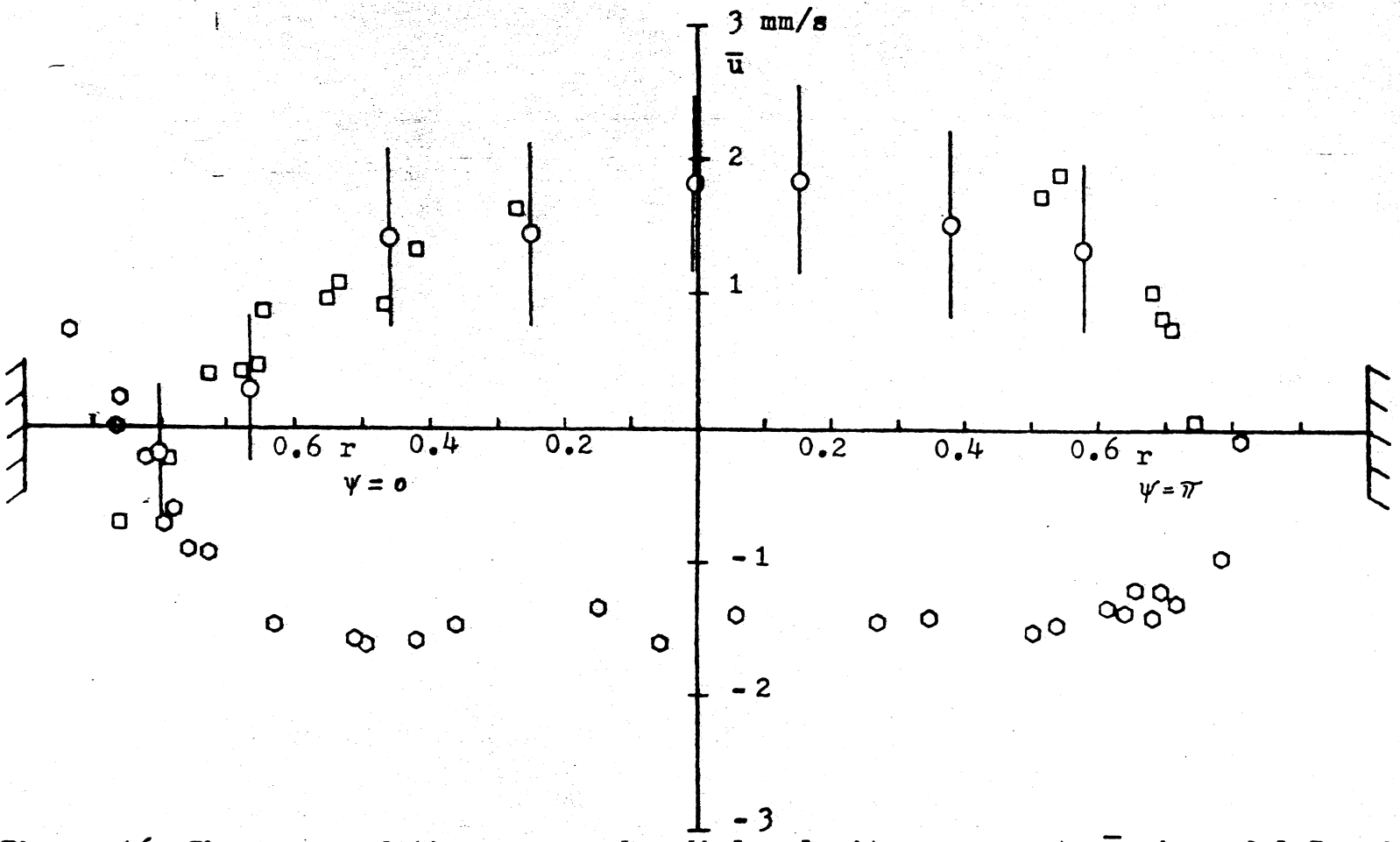

Figure 16. The measured time averaged radial velocity component $\bar{u}$ in model I and II, both with frequency f = 9Hz and in cross section 4 (other parameters, see figures 6 and 7, respectively). ○ and □ indicate measurements (photo) in model I and II, respectively. ◇, LDA measurements, model II.